MODELING DAMAGE MODES IN 3-D WOVEN ARMOR COMPOSITE SYSTEMS

R. Valisetty, A. M. Rajendran*, D. Grove, and R. Namburu
Comput. and Inform. Sciences Directorate, US Army Research laboratory
Aberdeen Proving Grounds, MD 21005
*Army Research Office, Research Triangle Park, RDU, NC

Y. Bahei-El-Din
Department of Mechanical, Aerospace & Nuclear Engineering
Rensselaer Polytechnic Institute, Troy, NY

A. Hody
Virginia Polytechnic Institute and State University, Blacksburg, VA

L. Seever
Embry-Riddle Aeronautical University, Daytona Beach, FL

ABSTRACT

In this paper a computationally intensive, multi-scale model exhibiting progressive damage in a 3D-woven composite is considered. It is based on evolving some fundamental damage modes in a representative volume element (RVE) of the composite's actual woven architecture. The evolving damage modes affect the local stresses in the composite micro-structure and eventually the overall stresses in the composite. This effect is considered in the RVE via a transformation field analysis (TFA). Since the model is computationally intensive, its numerical requirements in modeling the local micro-structure, e.g. the mesh size, are to be understood before it can successfully be used in armor lay-up design studies or in conjunction with Lagrangian impact codes such as DYNA3D. This is a convergence issue which has not been studied before in RVE-TFA theories which use separate meshes at local and global levels. This paper examines the effect of the local micro-mesh size on modeling the weave-level damage progression in the 3D-woven composites.

1. INTRODUCTION

Modern armor materials used in soldier protection gear and vehicle structures are essentially engineered materials. The material design process involves the selection of a geometric configuration (e.g., simple lay-ups, stitched/woven construction, etc.) consisting of appropriate combinations of material constituents (e.g., fibers, resins, particulates, etc.). This process can be overwhelming, because the selected armor design must perform under transient impacts in which the material constituents must deform and fracture in a controlled manner, i.e. the so called orderly progression of the local damage modes, to provide overall protection for the entire impact duration. Other than vast experimental data sets, no procedures are currently available to designers or material scientists that would tell them why certain combination of materials and geometry are better at providing overall protection, or how that protection might be achieved at the local level. Recent focus has been on the computational methods of overall impact response but not on how the local damage mode progression is affected by the built-up nature of the armor material design selection.

Since impact response includes shock propagation, large deformation, and brittle/plastic/viscous material behavior, theories used for selecting armor lay-ups must account for these effects. Such theories now are available for homogeneous materials only; procedures are available to extend them to composites but they suffer from the simplicity of material aggregation, i.e. the effects of individual material micro-phases and micro-damage average out. Accounting for such effects with continuously varying finite element meshes, i.e. a fine mesh at the micro-structural level that somehow transitions into a coarser one at the overall structure level, is also not feasible owing to the difficulties of computer storage, numerical instabilities, etc. These difficulties may be overcome through multi-scale analyses that employ separate meshes to describe local material micro-structures and the global macro-structures. One such theory by Bahei-El-Din (Bahei-El-Din et al., 2003) uses the transformation field analysis (TFA) of a representative volume element (RVE) of a 3D woven composite to model up to nineteen different modes of damage; each mode consists of either sliding, splitting, bulk, or tension failures of fiber, matrix and inter-phase materials. While multi-scale theories have been used before, the emphasis has been on the global response, i.e. very fine meshes in the global domain and very coarse meshes in the local micro domain. Even when large local meshes are used, allowing

Report Documentation Page

Form Approved
OMB No. 0704-0188

1. REPORT DATE	2. REPORT TYPE	3. DATES COVERED
01 NOV 2006	**N/A**	**-**

4. TITLE AND SUBTITLE	5a. CONTRACT NUMBER
Modeling Damage Modes In 3-D Woven Armor Composite Systems	5b. GRANT NUMBER
	5c. PROGRAM ELEMENT NUMBER
6. AUTHOR(S)	5d. PROJECT NUMBER
	5e. TASK NUMBER
	5f. WORK UNIT NUMBER
7. PERFORMING ORGANIZATION NAME(S) AND ADDRESS(ES) **Comput. and Inform. Sciences Directorate, US Army Research laboratory Aberdeen Proving Grounds, MD 21005**	8. PERFORMING ORGANIZATION REPORT NUMBER
9. SPONSORING/MONITORING AGENCY NAME(S) AND ADDRESS(ES)	10. SPONSOR/MONITOR'S ACRONYM(S)
	11. SPONSOR/MONITOR'S REPORT NUMBER(S)

12. DISTRIBUTION/AVAILABILITY STATEMENT
Approved for public release, distribution unlimited

13. SUPPLEMENTARY NOTES
See also ADM002075., The original document contains color images.

14. ABSTRACT

15. SUBJECT TERMS

16. SECURITY CLASSIFICATION OF:			17. LIMITATION OF ABSTRACT	18. NUMBER OF PAGES	19a. NAME OF RESPONSIBLE PERSON
a. REPORT	b. ABSTRACT	c. THIS PAGE			
unclassified	**unclassified**	**unclassified**	**UU**	**8**	

the elements to totally fracture and form debris clouds doesn't yield clues as to the underlying damage modes. By ignoring material fragmentation and damage mode interaction, the RVE-TFA method takes a mechanics based view of the developing damage modes, i.e. a damage mode once initiated will grow unhindered but controls the surrounding stress fields. The evolving stress field may further initiate damage elsewhere in the microstructure.

The earlier focus in the RVE-TFA work was on obtaining the local microscopic stresses and relating them to overall stress increments for conducting global-local modeling and on prallelizing the attendant computation (Valisetty et al., 2004). The parallelized computation enabled the consideration of larger local RVE meshes for a more realistic modeling of the local weave details, and the associated stress and strain fields, (Valisetty et al., 2005), but because the local RVE-TFA analysis are conducted at each and every global time step, the attendant RVE computations become time consuming placing a premium on the RVE mesh size. In spite of the fact that in RVE-TFA theories, the TFA, or the transformation field analysis, alludes to the step of re-adjusting the local stresses in response to locally spreading damage modes, the issue of RVE mesh size has not been studied in detail. Although some convergence was shown for the overall stresses and local RVE stress distributions, (Valisetty e al., 2007), the role of the RVE mesh size, i.e. how much it helps to have a larger mesh vs. a smaller one to model the locally spreading micro-damage has not been studied in detail. Results now are provided to show the progression of damage modes under the applied overall strain increments. By detailing the effect of local micro mesh size on the overall response as well as on evolutions of the local damage modes, the numerical underpinning for the RVE-TFA is computationally demonstrated.

2. RVE-TFA EQUATIONS FOR LOCAL STRESSES

RVE-TFA rests on the fact that an RVE can be used to model the point-wise variation of stress (or strain) fields in (a global Lagrangian analysis of a) composite as sums of elastic stresses that are computed directly from the applied overall loads and some self-equilibrating local transformation fields, i.e. which are significant within the the RVE. Each of the transformation fields can be associated with an on-going damage mode progression within the RVE; the magnitude of each one of such fields can be determined to keep the local stresses at levels to maintain an orderly progression of the damage modes as per some selected damage criteria; and the task of keeping the local RVE stresses at progressive damage levels has to be balanced out by adjusting the local stresses to restore local equilibrium. The TFA, or the transformation field analysis, refers to the last step of local RVE stress adjustment.

Fig. (1) shows a typical RVE used for a 3-D woven composite. Overall dimensions of the RVE are based on the dimensions apparent in the weave's micrograph. The number of sub-volumes in an RVE can be arbitrary but it is convenient to have each RVE sub-volume belonging to a distinct phase: fiber bundle, matrix, or interface.

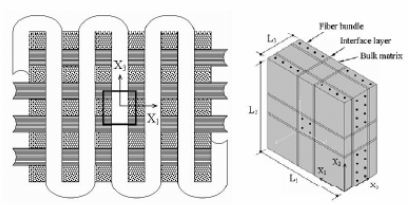

Fig. 1. A Schematic of a 3D woven composite and corresponding RVE

Original formulation of the TFA is due to Dvorak (1992) who later used the method for inelastic composite materials in Dvorak et al. (1994). Dvorak and Zhang (2001) used the TFA to analyze damage evolution in two-phase composites. Bahei-El-Din et al. (2004) extended the TFA method to the study of plate impact problems of 3-D woven composites by considering a full complement of damage modes including matrix and fiber cracking, fiber sliding, interface failure and debonding.

A brief summary of the relevant equations (Bahei-El-Din and Boutros, 2003) of TFA is presented below using a notation of boldface lower case letters for representing the (6x1) stress/strain vectors, and boldface upper case letters for the corresponding stiffness/compliance matrices. The global stresses/strains, $\overline{\sigma}$ and $\overline{\varepsilon}$, at an (integration) point where an RVE is used, are weighted volume sums of local sub-volume stresses and strains, σ_r and ε_r:

$$\overline{\sigma} = \sum_{r=1}^{Q} c_r \sigma_r , \qquad \overline{\varepsilon} = \sum_{r=1}^{Q} c_r \varepsilon_r , \tag{1}$$

where Q is the number of sub-volumes, c_r the sub-volume fractions. The local sub-volumes are assumed to undergo elastic deformation. Deviations from this mode of deformation are treated by adding transformation fields to account for the effects of temperature, shape, inclusions, plasticity, and damage. Symbolically, the local stresses/strains are expressed as follows:

$$\sigma_r = \mathbf{L}_r \varepsilon_r + \lambda_r , \qquad \varepsilon_r = \mathbf{M}_r \sigma_r + \mu_r , \tag{2}$$

where $\mathbf{L}_r$ and $\mathbf{M}_r = \mathbf{L}_r^{-1}$ are elastic stiffness and compliance, μ_r and $\lambda_r = -\mathbf{L}_r \mu_r$ are transformation strains and stresses. A part of the local sub-volume stresses/strains can be related to the global applied loads following the treatment of elastic composite aggregates

by Hill (1963, 1965), and the rest to a superposition of all the transformation fields originating in all local sub-volumes within the RVE, Dvorak (1992) as

$$\varepsilon_r = \mathbf{A}_r \bar{\varepsilon} + \sum_{s=1}^{Q} \mathbf{D}_{rs}\mu_s \,, \quad \sigma_r = \mathbf{B}_r \bar{\sigma} + \sum_{s=1}^{Q} \mathbf{F}_{rs}\lambda_s \,, \qquad r = 1,\ldots,Q, \quad (3)$$

where $\mathbf{A}_r$ and $\mathbf{B}_r$ are stress/strain concentration factors, $\mathbf{D}_{rs}$ and $\mathbf{F}_{rs}$ are transformation influence factors for the r^{th} local sub-volume. All these factors depend upon the RVE local geometry and properties of the local phases and can be determined from an elastic analysis of the RVE mesh. The concentration factors are computed as statically equivalent to the global stresses available on the RVE. For example, the k^{th} column, k=1,…,6, of the stress concentration factor, $\mathbf{B}_r$, r = 1, 2,…,Q, is computed by giving a unit value to the k^{th} stress component and 0 to the rest of the 6x1 overall stress vector, $\bar{\sigma}$. This is done in the usual finite element sense by assuming a linearly varying local displacement field in the RVE, and by securing the RVE against rigid body deformation, (Dvorak and Teply, 1985).

A similar procedure is also used for computing the transformation influence factors by realizing that a k^{th} column, k=1,2,…,6, of $\mathbf{F}_{rs}$, r,s=1,2,…,Q, is a response in the sub-volume V_r after a unit stress, $\lambda_k = 1$, is applied in the sub-volume V_s. A total of 6Q RVE finite element solutions are required to completely evaluate the transformation factors. Since the RVE stiffness matrix remains the same, the only variants are the effective loads on the right hand side. Now the equations for computing the overall response in terms of local stresses/strains are presented. Following Eq. (1), these are symbolically represented as

$$\bar{\sigma} = \bar{\mathbf{L}}\bar{\varepsilon} + \bar{\lambda} \,, \quad \bar{\varepsilon} = \bar{\mathbf{M}}\bar{\sigma} + \bar{\mu} \qquad (4)$$

where $\bar{\mathbf{L}}$ and $\bar{\mathbf{M}} = \bar{\mathbf{L}}^{-1}$ are overall elastic stiffness and compliance matrices. The overall transformation fields are related by

$$\bar{\lambda} = -\bar{\mathbf{L}}\bar{\mu} \,. \qquad (5)$$

By substituting the results of Eqs. (2) and (5) into Eq. (1), the overall elastic stiffness and compliance matrices are evaluated as

$$\bar{\mathbf{L}} = \sum_{r=1}^{Q} c_r \mathbf{L}_r \mathbf{A}_r \,, \qquad \bar{\mathbf{M}} = \sum_{r=1}^{Q} c_r \mathbf{M}_r \mathbf{B}_r \qquad (6)$$

The overall transformation fields also are provided by Levin's (1967) equations (Dvorak, 1992), as

$$\bar{\lambda} = \sum_{r=1}^{Q} c_r \mathbf{A}_r^T \lambda_r \,, \qquad \bar{\mu} = \sum_{r=1}^{Q} c_r \mathbf{B}_r^T \mu_r \,. \qquad (7)$$

3. DAMAGE MODES AND PROGRESSION

In the RVE-TFA formulation described so far, the problem is reduced to finding the local transformation fields. When local constituents' are elastic, there is no need for the transformation fields. When materials are inelastic, the transformation fields can be used to offset the local RVE stresses from their elastic values to restore local yield criteria, in the sense of radial return plasticity. In a similar manner, specific damage modes are also handled. For example, Bahei-El-Din (1996), Dvorak and Zhang (2001) and Bahei-El-Din and Botrous (2003) treated the interfacial debonding stresses as transformation fields, and applied them as equivalent nodal forces to the RVE.

For an RVE of a composite which is discretized into Q sub-volumes, $V_\rho, \rho = 1,2,...,Q$, the undamaged local or elastic stresses are found from the stress concentration factors, $\mathbf{B}_r$ and either the applied overall stress as $\mathbf{B}_r \bar{\sigma}$, or the overall applied strain as $\mathbf{B}_r \mathbf{L} \bar{\varepsilon}$. Suppose now there is some progressing damage in one or many sub-volumes, $V_\rho, \rho = 1,2,...,Q^*, Q^* \le Q$, of the RVE. The computed elastic stresses then will exceed the underlying strength values in some of those sub-volumes. One or several damage modes may be progressing in those sub-volumes. Then to bring the computed elastic stresses to conform with the requirements for an orderly progression of each and every one of the progressing damage modes, transformation stress fields, equal in number to those causing the progressing damage modes, are introduced and evaluated. The equations are described next to enable the computation of actual stresses in the RVE sub-volumes in the presence of progressing damage modes. Essentially, these equations are statements that the sums of the elastic stresses and the transformation stresses, i.e. the local stresses, should be set at values as required by the damage criteria for the involved damage modes. This may result in the development of damage in new sub-volumes and as such the process is repeated to compute the local stresses in the presence of all possible damage modes caused under the applied overall load.

The transformation fields are evaluated by recasting Eq. (3). This is done by recognizing that the first parts on the right hand side of the equations, i.e. Eq. $(3)_1$, are the elastic stresses and the second parts, i.e. Eq. $(3)_2$, are the transformation fields, and together these two parts equal to the current local stresses on the left hand side of Eq. (3). The transformation fields are evaluated by setting the current stresses on the left hand side at values that can be sustained in the presence of progressing damage modes.

To present the equations, and later damage modes and their growth and criteria, local stresses are considered in local coordinate systems with appropriate co-ordinate

transformation matrices, $\mathbf{R}_\rho$. The local coordinate systems are not unique; they change depending on sub-volume phase orientations and the specific damage criteria. Referring to such local coordinate systems and using stress ratios, $\varphi_k^{(\rho)}$, which are current stresses divided by their elastic undamaged values, the equations for computing transformation stress are presented as (Bahei-El-Din et al., 2004):

$$\sum_{\eta=1}^{Q^*} \mathbf{F}_{\rho\eta}\,\mathrm{diag}(\alpha_k)\lambda_\eta = -\mathbf{I} - \mathbf{R}_\rho^{-1}\,\mathrm{diag}(\varphi_k^{(\rho)})\mathbf{R}_\rho)\mathbf{B}_\rho\,\overline{\sigma},\ \rho=1,2,,,Q^*, \tag{8}$$

$$\alpha_k = \begin{cases} 1 \text{ if } 0 \le \phi < 1 \\ 0 \text{ if } \phi = 1 \end{cases}, \tag{9}$$

where diag(x) is a (6x6) matrix. The stress ratios, $\varphi_k^{(\rho)}$, k=1,2,...,6, $\rho=1,2,...,Q^*$, $Q^* \le Q$, imply pre- and post-damage loading as follows: $\varphi_k^{(\rho)}=1$ for a stress component that has yet not violated the onset of damage, $\varphi_k^{(\rho)}=0$ indicates complete unloading, and $0 \le \varphi_k^{(\rho)} \le 1$ indicates progressing damage with partial property decay. If $\varphi_k^{(\rho)}<1$ for all k=1,2,…,6 and for all Q^* sub-volumes, then there are $6\,Q^*$ equations in Eq. (8) for evaluating the transformation fields. If some of the local stress components are unaffected by the underlying damage criteria, the corresponding stress ratios would equal unity. In such cases $\alpha_k=0$, and the corresponding transformation stresses will not be needed and enough equations will drop out from Eq. (8). The equations available after this consideration are solved for the transformation stresses that are remaining.

3.1 Damage modes

Although the RVE-TFA analysis is completed by updating the local sub-volume stresses with contributions from the transformation stress fields and by computing the overall stresses and stiffness properties, etc., its description here is not complete without mentioning the specific damage mechanisms that are considered in this work. The RVE-TFA code (Bahei-El-Din et al, 2004) considers damages of fiber bundles, interface layers, and matrix but specializes the progression of these damages on planes specific to 3-D woven fabrics. Specific damage modes are considered in each material system. Four damage modes are considered in the fiber bundles as follows: longitudinal fiber rupture, transverse inter-bundle fiber sliding, longitudinal inter-bundle fiber sliding, and transverse inter-bundle fiber splitting. Two damage modes are considered in the interface layers as follows: shear sliding and peeling. The bulk matrix damage is assumed to be terminal, i.e. without any recovery.

Some of these damage modes interact with each other and while others do not. For example, $\hat{\sigma}_{22}, \hat{\sigma}_{33}, \hat{\sigma}_{23}$, the stresses resolved in a co-ordinate frame aligned with the axis of a fiber bundle, affect fiber bundle sliding and splitting. Therefore, these modes are deemed interactive. On the other hand, the two interface layer damage modes do not interact, and these are deemed independent. The stress ratios, φ_k, which are introduced to keep track of the damage progression, become unique and independent when the corresponding damage modes do not interact; while the stress ratios involved in the interacting damage modes are not unique. For such interacting modes, the stress ratio which controls the weakest of the interacting sub-damage modes is selected.

3.2 Damage Progression

The damage progression is implemented next with the aid of the post-elastic material behavior of the RVE sub-volumes and interpreted with the aid of numerical loading. The stress and strain allowables curve is assumed in the form of (*s*,*e*) using scalars quantities that can be computed with the knowledge of the local stresses and the damage modes. This curve is initially assumed to be linear, until the ultimate stress and the corresponding elastic strain limits are reached (s_{ult}, e_{el}). It is later assumed to show softening. The softening branch is assumed to take a linear or a nonlinear form, defined symbolically as $s=g(e-e_{el})$, where $e_{el} \le e \le e_{ult}$, and e_{ult} is the ultimate strain. Unloading/reloading follows a linear path between the origin and the (*s*,*e*) curve.

For a given strain $e^{(i)}$, at the ith numerical loading step of the applied load, the elastic stress is computed as $s^{(i)}=(s_{ult}/e_{el})e^{(i)}$, which may or may not fall on the allowable (*s*,*e*) curve. The correct stress magnitude, and hence the current stress ratio, $\varphi^{(i)}$, is determined to match the allowable from the (*s*,*e*) curve and the values of $s^{(i)}$, $e^{(i)}$, and $\varphi^{(i-1)}$, the stress ratio at the previous step, as follows:

$$\begin{aligned} &\text{undamaged state}: \varphi^{(i)}=1, \quad \text{if } \varphi^{(i-1)}=1,\ 0 \le e^{(i)} < e_{el} \\ &\text{damage reversal}: \varphi^{(i)}=\varphi^{(i-1)}, \text{ if } \varphi^{(i-1)}<1,\ 0 \le e^{(i)} < e_{el} \end{aligned}, \tag{10}$$

$$\begin{aligned} &\text{continued damage}: \\ &\varphi^{(i)} = \frac{g(e^{(i)}-e_{el})}{s^{(i)}}, \text{ if } \frac{g(e^{(i)}-e_{el})}{s^{(i)}} < \varphi^{(i-1)}, e_{el} \le e^{(i)} < e_{ult} \\ &\text{damage reversal}: \\ &\varphi^{(i)} = \varphi^{(i-1)}, \text{if } \frac{g(e^{(i)}-e_{el})}{s^{(i)}} > \varphi^{(i-1)}, e_{el} \le e^{(i)} < e_{ult} \end{aligned}. \tag{11}$$

The 1st condition in Eq. (10) represents the response of an undamaged material, while the 1st condition in Eq. (11) describes continued loading of a previously damaged

state. The remaining conditions above represent linear unloading/reloading from a damaged state. Hence, damage is recorded during the loading history through the incremental values of the stress ratio $\varphi_k^{(i)}$.

The stress and strain pair at the current loading step $(s^{(i)}, e^{(i)})$, has different interpretations depending on the type of the RVE constituent and the associated damage mode. In what follows, these quantities are related to the local stress and strain averages for a fiber bundle, the bulk matrix, and the matrix interface layers. It is assumed that the total overall stress $\bar{\sigma}^{(i)}$ at the current loading step is known, either directly by following a defined, stress-controlled loading path, or as the stress $\mathbf{B}_r \mathbf{L}\, \bar{\varepsilon}^{(i)}$ caused in an undamaged RVE by a strain-controlled loading,. The corresponding local stress in a sub-volume $V_\rho, \rho = 1,2,...,Q$, of the RVE, can then be found from the first term of Eq. $(3)_2$. When this is transformed to the local coordinates of the sub-volume, and the result is substituted into the first term of Eq. $(2)_2$, the local stress, $\hat{\bar{\sigma}}_{rr}$, and strain, $\hat{\bar{\varepsilon}}_{rr}$, described in the local coordinate system of the sub-volume, are found at loading step (i) as

$$\hat{\sigma}_r^{(i)} = \mathbf{R}_r \mathbf{B}_r \bar{\sigma}^{(i)},\ \hat{\varepsilon}_r^{(i)} = \hat{\mathbf{M}}_r \hat{\sigma}_r^{(i)},\ r = 1,2,...,Q \ . \qquad (12)$$

Matrix $\mathbf{R}_r$ relates the stresses described in the local and the overall coordinate systems, and $\hat{\mathbf{M}}_r$ is the elastic compliance described in the local axes. Expressions for evaluating $s^{(i)}$ in terms of the resolved stress $\hat{\sigma}$ and material properties e_{el}, e_{ult}, s_{ult} for the above listed damage conditions follow composite material mechanics damage concepts. The specific ones used in this study are from Bahei-El-Din et al., 2004.

4. RESULTS

In this section, numerical results are presented to show the convergence for the local damage progression with respect to the increasing local RVE mesh sizes.

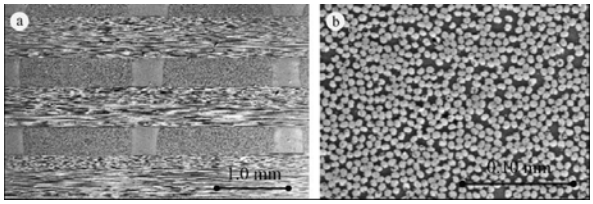

Fig. 2. Cross-sections through (a) the warp fiber bundle and (b) through the weft fiber bundle.

For this purpose, a 3D woven composite made of S2 glass/epoxy system is considered. The composite was evaluated to have the micro-geometry shown in Fig. 2. As seen in the micrographs of Fig. (2a), the fiber bundles in the warp and weft directions have a rectangular cross-section with aspect ratio of about 4.0, while the z-fiber bundle has a square cross-section. For the composite, a simple RVE idealization with an approximate material placement of the fiber bundles in the warp, weft and z directions, and the resin and interfacial layers is considered shown in Fig. $(1)_2$. The dimensions of the RVE parallel to the overall in-plane axes were taken as 12mm and 12mm, and in the z-direction as 2.2mm.

For fiber bundles, the following properties are used: E_L=59.7 GPa, E_T=11.7 GPa, ν_{LT}=0.248, ν_{TT}=0.371, G_{LT}=5 GPa, G_{TT}=4.68 GPa, σ_{max}-$_L$=3.36 GPa, γ_T=0.0112, $\sigma_{max\text{-}T}$=0.08 GPa, ε_T=0.0068, $\varepsilon_{max\text{-}T}$=0.0068, $\tau_{max\text{-}L}$=0.057 GPa, $\tau_{max\text{-}T}$ = 0.048 GPa, γ_L=0.0114, $\gamma_{max\text{-}L}$=0.0114, $\tau_{max\text{-}T}$=0.048GPa, $\gamma_{max\text{-}T}$=0.0112, where E, G, ν, σ, τ, ε and γ are Young's modulus, shear modulus, Poisson ratio, normal stress, shear stress, normal strain and shear strain, respectively, and subscripts L and T indicate longitudinal and transverse directions. For the matrix, the following properties are used: E=2.9 GPa, =0.3, σ_{max}=0.06 GPa, ε_{max}=0.021, τ_{max}=0.035 and γ_{max} =0.0313.

Having thus developed the RVE of Fig. $(1)_2$, it is used for the mesh size convergence study. To begin the study, several RVE meshes were considered as shown in Fig. (3). Once again several possibilities existed for increasing the sub-volumes, but the indicated pre-ponderance of sub-volumes in the z-direction was in view of the intended application of RVE-TFA in composite armor impact design studies.

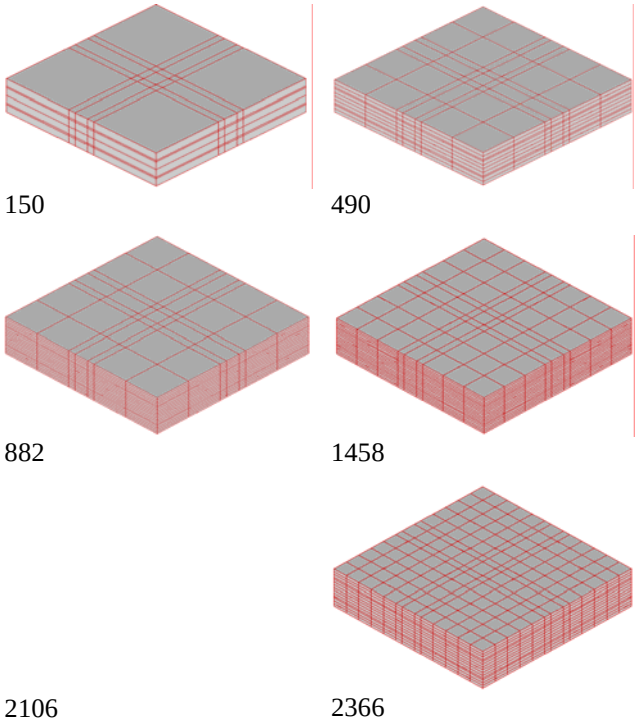

Fig. 3. Different finite element meshes for the RVE

In this study, a unit RVE cell was subjected to the following overall strains separately and incrementally: $\bar{\varepsilon}_{11}$, $-\bar{\varepsilon}_{11}$, $\bar{\varepsilon}_{33}$, $-\bar{\varepsilon}_{33}$, $\bar{\gamma}_{12}$, and $\bar{\gamma}_{13}$. For these loadings, TFA analyses were conducted and results were generated for the overall stress vs. strain curves and local stress distributions in the RVE. These results, presented in Valisetty et al., 2005 and 2007, showed convergence for the local stress distributions, the overall stresses and failure limits on the overall stresses and strains with respect to the increasing mesh size and led to a conclusion that an RVE mesh of 490 is adequate to generate the RVE's overall response. The analyses also gave information on the damage modes that became active as the overall strains were incremented. These results are presented in this paper.

In the RVE-TFA, the progression of damage modes is considered indirectly by letting the progressing damage modes control the local stresses and by keeping track of the local sub-volumes in which specific damage modes were active. In Fig. (4)-(9), overall stress vs. (applied overall) strain plots are superimposed by the plots of individual counts of the failing sub-volume accumulations vs. the applied overall strains for each of the active damage modes. The damage modes that spread to most sub-volumes by the earliest applied overall strain are considered dominant and are listed.

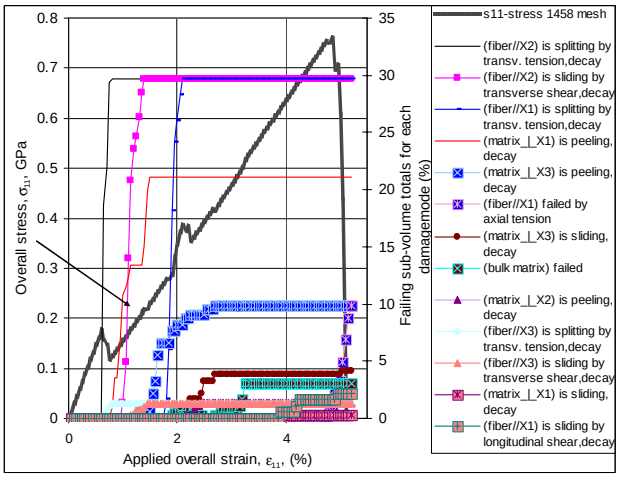

Fig. 4. Eff. of progressing damage modes on $\bar{\sigma}_{11}$ vs. $\bar{\varepsilon}_{11}$

For the in-plane tensile loading, Fig. (4), several damage modes appear but the dominant ones in the order of their rapid growth may be listed as: fiber splitting normal to the load direction, fiber sliding due to transverse shear decay, fiber sliding due to transverse tension, matrix peeling, etc. The important fiber failure due to axial tension doesn't become significant until the applied strain reaches 4.75% after which the overall stress drops precipitously. For the in-plane compressive loading, Fig. (5), the dominant damage modes are all related to the fiber sliding. Since it was assumed that the fiber bundle does not fail under compression, at least in the 0 to 8% strain range that was investigated, the stress keeps raising after the initial matrix bulk matrix failure.

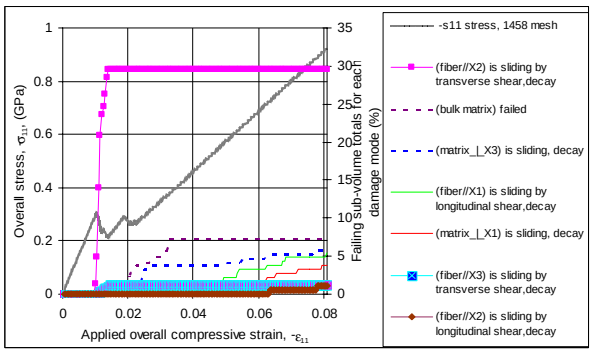

Fig. 5. Eff. of progressing damage modes on $-\bar{\sigma}_{11}$ vs. $-\bar{\varepsilon}_{11}$

For the out-of-plane normal tensile loading, Fig. (6), as expected, the only active damage mode is matrix peeling and it brings down the stress precipitously. For the out-of-plane normal compressive loading, Fig. (7), the damage modes are related to fiber bundle sliding due to transverse shear decay, and these modes too bring down the stress precipitously.

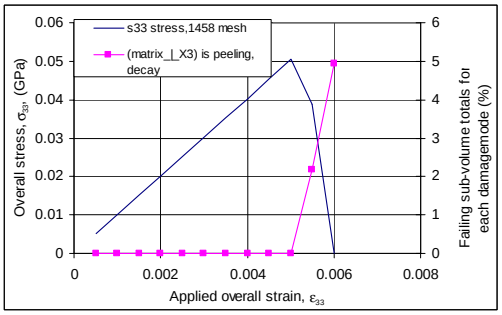

Fig. 6. Eff. of progressing damage modes on $\bar{\sigma}_{33}$ vs. $\bar{\varepsilon}_{33}$

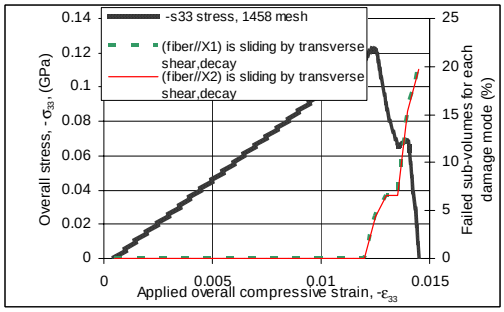

Fig. 7. Eff. of progressing damage modes on $-\bar{\sigma}_{33}$ vs. $-\bar{\varepsilon}_{33}$

For the in-plane shear loading, Fig. (8), the bulk matrix failure appears at the earliest. It is followed by the fiber bundle sliding modes parallel to the out-of-plane axis, but the eventual stress drop-off occurred due to the

sliding caused by the longitudinal shear in the warp and weft fiber bundles. For the out-of-plane shear loading, Fig. (9), the bulk matrix failure and the fiber sliding damage modes appear earlier but the eventual stress loss is precipitated by the matrix sliding damage mode.

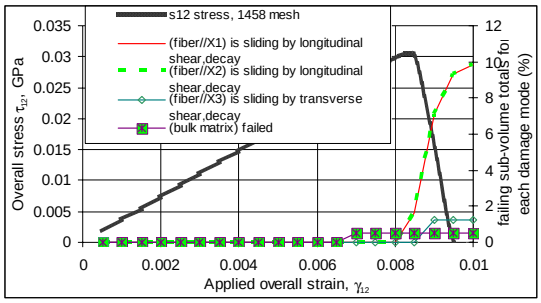

Fig. 8. Effect of progressing damage modes on $\bar{\tau}_{12}$ vs. $\bar{\gamma}_{12}$

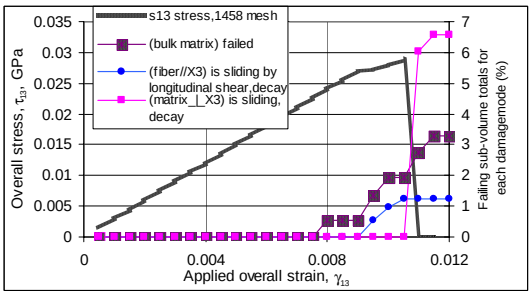

Fig. 9. Effect of progressing damage modes on $\bar{\tau}_{13}$ vs. $\bar{\gamma}_{13}$

The appearance and growth details of the individual damage modes are important in fine tuning the individual constituents of the composite. Although the direct strength properties are important, the failures due to sliding indicate the preponderance of transverse shear failures which may be improved by modifying the resin characteristics. In Figs. (4)-(9), the results from the 1458 sub-volume RVE micromesh are used for the overall stress vs. strain curves, and for the sub-volume counts for the individual damage modes. Similar trends are also found for other RVE mesh sizes, and in Figs. (10)-(15), the totals of the counts of sub-volumes that are affected by all the damage modes are presented vs. the respective applied strains.

As can be seen in Fig. $(10)_1$, all the RVE mesh sizes show the same growth trend for the totals of the damage affected sub-volumes with respect to the applied in-plane normal strain. Similar conclusion also can be inferred from the results for the total accumulations of damaged sub-volumes under the in-plane compressive normal strain loading in Fig. $(10)_2$.

The totals of the damage affected sub-volumes are presented with respect to the applied out-of-plane normal strain, in Fig. (11). The results for longitudinal shear loading and transverse shear loading are shown in Fig. (12)-(13), respectively. All these loading cases are matrix dominated. The strain range in which the first damage mode appears and the eventual stress loss occurs is small ~ 0.1%. Similarly the number of sub-volumes available for the spread of the damage, i.e. the number of interface sub-volumes, is also limited. This explains the variation found in the predictions by the different RVE meshes for these loading cases. Even then all the RVE meshes show identical damage modes and their onset at approximately same applied strain values.

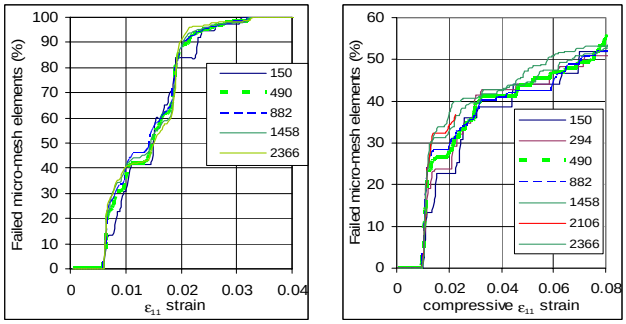

Fig. 10. Mesh effect on the accumulation of all damaged sub-volumes under in-plane normal loading

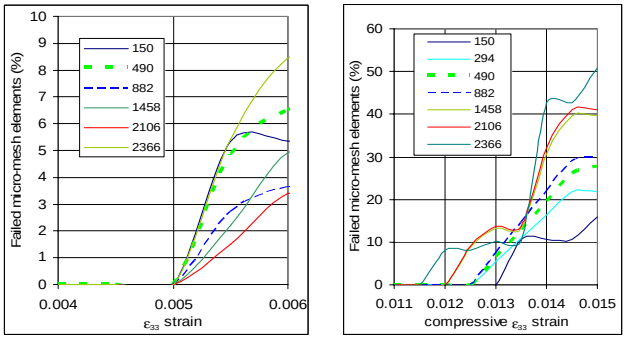

Fig. 11. Mesh effect on the accumulation of damaged sub-volumes under out-of-plane normal loading

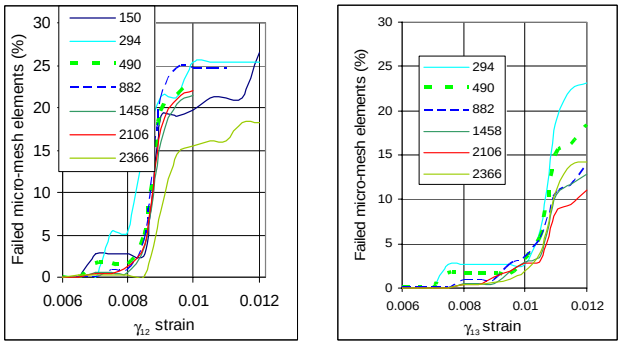

Fig. 12. Mesh effect on the accumulation of damaged sub-volumes under shear loadings.

Based on the results presented in two earlier publications for the overall stresses vs. overall strains and local stress distributions and the results presented in this paper for the on-set and progression of the local damage modes, an RVE mesh size ~490 can also be deemed to be sufficient to approximately describe both the stress picture and the spreading damage in the RVE at the composite weave level and thus can be suitable for conducting RVE based 3-D woven composite design studies.

5. CONCLUSIONS AND FUTURE WORK

A physically based material model of a 3D woven composite is investigated for the requirement of the mesh size of its representative volume element (RVE) to capture the underlying weave details and the locally spreading damage modes. The damage modes considered are typical of those observed in quasi-static and impact tests of woven composite samples, and include matrix cracking, frictional sliding and debonding of the fiber bundles, and fiber rupture. The local stresses are obtained using a transformation field analysis (TFA) as sums of the elastic, undamaged response and the contributions of an auxiliary transformation stress fields to correct for the selected damage modes.

A wide range of mesh sizes were considered for these RVE's to capture the locally spreading damage modes. The progressions of damage modes were considered indirectly by letting the progressing damage modes control the local stresses in the RVE sub-volumes and using accumulations of such sub-volumes as a measure of the spread of the local damage modes. The computed response includes the local and overall stresses, as well as the on-set and progression of the local damage modes.

As the results presented in two earlier publications for the overall stresses vs. overall strains and local stress distributions and the results presented in this paper for the on-set and progression of the local damage modes show, all the RVE mesh sizes above 150 are capable of recording, within an acceptable range, both the overall stresses and the accumulations of the locally damaged sub-volumes under simple overall strain loading conditions. However, to generalize the central conclusion of this study that a reasonable RVE mesh size ~490 can be set needs further evaluation possibly for additional applied strain regimes, un-loading/re-loading paths, dynamic impact, and additional weave architectures as well as material systems.

ACKNOWLEDGEMENTS

This work was supported by a grant of computer time from the DOD High Performance Computing Modernization Program at the US Army Research Laboratory, Major Shared Resource Center, Aberdeen Proving Ground, MD, USA.

REFERENCES

Bahei-El-Din, Y. A.,1996: Finite Element Analysis of Viscoplastic Composite Materials and Structures. Mech Comp Mat Struc 3, 1-28.

Bahei-El-Din, Y. A., and Botrous, A. G., 2003: Analysis of Progressive Fiber Debonding in Elastic Laminates. Int J Solids Struc, 40, 7035.

Bahei-El-Din, Y. A., Rajendran, A.M. and Zikry, M. A, 2004: A micromechanical model for damage progression in woven composite systems. *International Journal of Solids and Structures* 41, 2307.

Dvorak, J. J. and Teply, J. L., 1985: Periodic Hexagonal Array Models for Plasticity Analysis of Composite Materials. In: Plasticity Today: Modeling, Methods and Applications, Sawczuk, A. and Bianchi, V., editors, W. Olaszak Memorial Volume, Elsevier Scientific Publishing Co., Amsterdam, pp. 623-642.

Dvorak, G. J., 1992: "Transformation Fields Analysis of Inelastic Composite Materials," *Proceedings of the Royal Society* A437, 311.

Dvorak, G. J., Bahei-El-Din, Y.A. and Wafa, A. M., 1994: *Computational Mechanics* 14, 201.

Dvorak, G.J. and Zhang, J., 2001: *Journal of the Mechanics and Physics of Solids* 49, 2517.

Hill, R., 1963. Elastic properties of reinforced solids: some theoretical principles. J. Mech. Phys. Solids 11, 357–372:

Hill, R., 1965. A self-consistent mechanics of composite materials. J. Mech. Phys. Solids 13, 213–222.

Levin, V.M., 1967: Thermal expansion coefficients of heterogeneous materials. Mech. Solids 11, 58–61.

Valisetty, R., Namburu, R., Rajendran, A. M. and Bahei-El-Din, Y. A., 2004: "Scalable coupling of TFA and PARADYN analyses for impact modeling of 3-d woven composites," Proceedings of the 2004 International Conference on Computational & Experimental Engineering & Sciences ISBN: 0-9657001-6-X2004, Tech Science Press, pp 92-97.

Valisetty, R., Namburu, R., Rajendran, A. M., Bahei-El-Din, Y. A., Hody, A. and Seever, L., 2006: "Scalable RVE pre-processor for TFA analysis OF 3-D woven composite impacts," Submitted for publication as an ARL report.

Valisetty, R., Namburu, R., Rajendran, A. M. and Bahei-El-Din, Y. A., 2007: "Mesh size effect in RVE-TFA modeling of 3-D woven composites," Submitted for publication to ICCES 2007.